# Time-domain Ramsey-narrowed sub-kHz electromagnetically induced absorption in atomic potassium



OPEN ACCESS
IOP Publishing
Journal of Physics B: Atomic, Molecular and Optical Physics
J. Phys. B: At. Mol. Opt. Phys. **52** (2019) 085002 (7pp)
https://doi.org/10.1088/1361-6455/ab0fc5

# Time-domain Ramsey-narrowed sub-kHz electromagnetically induced absorption in atomic potassium

**Lorenzo Lenci[1], Luca Marmugi[2,3], Ferruccio Renzoni[2], Silvia Gozzini[3], Alessandro Lucchesini[3] and Andrea Fioretti[3]**

[1] Facultad de Ingeniería, Instituto de Física, Universidad de la República, J. Herrera y Reissig 565, 11300 Montevideo, Uruguay
[2] Department of Physics and Astronomy, University College London, Gower Street, London WC1E 6BT, United Kingdom
[3] Istituto Nazionale di Ottica, INO-CNR, Sede Secondaria di Pisa, Via Moruzzi 1, I-56124 Pisa, Italy

E-mail: l.marmugi@ucl.ac.uk

Received 28 December 2018, revised 12 February 2019
Accepted for publication 14 March 2019
Published 2 April 2019

**Abstract**

The use of electromagnetically induced absorption (EIA) in sensing and metrology has been thus far hindered by saturation effects, which severely degrade its linewidth. Here we propose, and experimentally demonstrate, that time-dependent Ramsey spectroscopy in potassium vapour overcomes the detrimental effect of saturation. We observe sub-kHz Ramsey fringes, with full control of the EIA resonance characteristics. Combined with the efficient optical pumping associated to the K $D_1$ line, the present work demonstrates an EIA scheme suitable for sensing and metrological applications.

Keywords: electromagnetically induced absorption, Zeeman effect, line shapes and shifts, Ramsey fringes

## 1. Introduction

Atomic gases, both at ultracold and at room temperatures, have become an important resource in metrology and sensing, from atomic clocks [1] to atomic magnetometers [2]. Their use rely on optical resonances, whose width is a critical parameter. Ground state resonances are particularly appealing in this context, as their long lifetime allows for the observation of ultra-narrow spectral features. Coherent population trapping (CPT) [3–5] resonances in alkali atoms are of particular relevance for metrological and sensing applications, given their sub-natural linewidths, as small as a few tens of Hz [6, 7]. This feature has led to the realisation of CPT-based atomic clocks [8] and magnetometers [9, 10]. An alternative approach is electromagnetically induced absorption (EIA) [11–14], whose resonances also exhibit sub-natural linewidth. However, detrimental saturation effects associated to optical pumping severely degrade its linewidth: EIA resonances only down to the kHz range or above have been reported [15–18]. *Spatial* Ramsey-induced narrowing for coherent resonances was also demonstrated [19–22].

In this work, we propose and demonstrate an experimental protocol for EIA which overcomes the limitations that have been hindering high-resolution applications thus far. By applying a *time-dependent* Ramsey excitation scheme to $^{39}$K thermal vapour prepared in an EIA configuration, we circumvent the saturation broadening effects [23] that degrade the EIA linewidth, to observe sub-kHZ Ramsey-narrowed EIA resonances. In our scheme, $^{39}$K is optically pumped to a stretched state with an intense laser pump tuned to the $D_1$ line. This creates an imbalance in the atomic populations, producing the conditions for EIA [24, 25] in a transverse magnetic field. After free evolution, when the atomic population oscillates between the Zeeman sublevels of the atomic ground states, the system is probed by a second laser beam, which



 

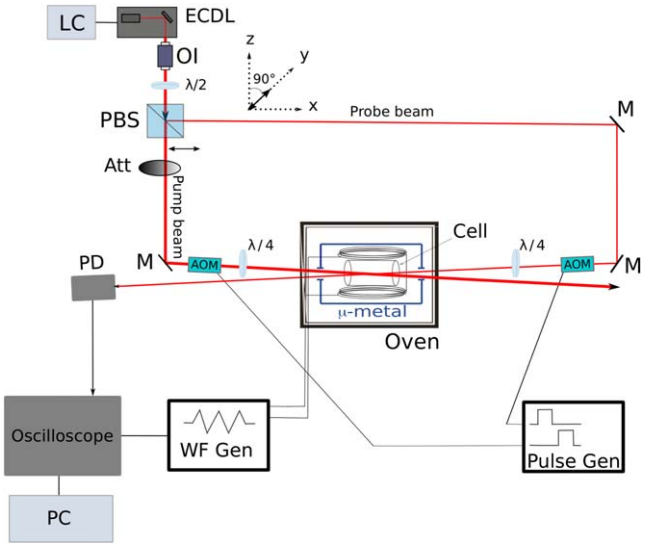


**Figure 1.** Sketch of the experimental setup. LC: laser controller. ECDL: extended-cavity diode laser. OI: optical isolator. $\lambda/2$, $\lambda/4$: half- and quarter-waveplates, respectively. PBS: polarising beam splitter. M: mirror. Att: variable attenuator. PD: photodiode. AOM: acousto-optic modulator. WF, Pulse Gen: waveform and pulse generator, respectively.

exhibits enhanced absorption modulated by the Ramsey oscillations. The overlapping of Ramsey fringes to the EIA resonance produces a controllable large reduction of its linewidth, down to 130 Hz (half width at half maximum (HWHM)).

Our approach relies on two main advantages. (i) The K hyperfine structure allows more efficient optical pumping, thus enhancing the atomic state preparation of EIA [15]. This would not be possible in other alkalis, where the hyperfine splitting (hfs) exceeds the Doppler width of the ground state transitions [26]. (ii) The temporal separation of pump and probe realised in the Ramsey scheme allows the use of intense pump, as required for efficient optical pumping. This does not affect the EIA resonance linewidth. Similarly, a reduction of light shift [27] in EIA-based frequency standards can be obtained. In this way, we bring applications of EIA in sensing and metrology closer.

## 2. Experimental setup

The experimental arrangement is sketched in figure 1.

K vapour, a mixture of $^{39}$K (93%), $^{41}$K (7%) vapour and 5 Torr of Ar buffer gas, is contained in a polydimethylsiloxane (PDMS) coated glass cell, of 22 mm diameter and 48 mm length. The buffer gas prevents quick escape of the atoms from the interaction volume, and reduces the likelihood of depolarising alkali/alkali collisions, while enhancing that of velocity-changing collisions. Organic coatings prevent spin relaxation upon atom/wall collisions [28]. These characteristics allow atoms to fully exploit the overlapped hyperfine structure of the ground state. The vapour cell is enclosed in a single layer of mu-metal, which reduces the effect of stray magnetic fields. A pair of Helmholtz coils is placed inside the shield, to apply a magnetic field perpendicular to the laser beams ($B_\perp$). The transverse magnetic field is swept around $B_\perp = 0$ by a triangular waveform. A heater, positioned externally to the shield and in contact with it, maintains the cell at 45 °C. Three pairs of coils, two in Helmholtz configuration, one in anti-Helmholtz, are placed outside the mu-metal to compensate for residual Earth and stray magnetic fields and for gradients along the cell axis, respectively.

Atoms interact with a counter-propagating pair of pump and probe beams, generated by the same laser source (Toptica DL100, linewidth $<1$ MHz), tuned to the $D_1$ line of $^{39}$K at 770.1 nm. Both beams are circularly polarised, with equal handedness, thus producing a $\sigma^+$–$\sigma^-$ excitation in the atomic reference frame. The beam waists of the pump and probe beams are 2.3 mm and 1 mm, respectively. Each beam is independently pulsed by an acousto-optic modulator (AOM), acting as fast switch. AOMs are controlled by programmable delay lines. Absorption of the probe beam is measured by a fast photodiode, connected to a digital oscilloscope (Lecroy Waverunner 64XI, 8 bit).

EIA is observed as a function of $B_\perp$, in degenerate conditions, with the optimum tuning of the ECDL laser [15]. In detail, atoms are optically pumped in the stretched state $|F = 2, m_F = -2\rangle$. For $B_\perp \neq 0$, coherent mixing of the ground state Zeeman sublevels is produced. This evolves in a maximally absorptive state at $B_\perp = 0$, with the appearance of an EIA resonance, due to population redistribution. In this sense, EIA is here produced by transfer of population [24]. As recently observed, the specific features of the K $D_1$ hyperfine structure and the realised excitation scheme increase the efficiency of optical pumping and therefore of EIA [15]. Specifically, given the K small hfs (461.7 MHz and 57.7 MHz for ground and excited state, respectively) compared to the Doppler linewidth (797 MHz at 45 °C [29]), there is a substantial overlapping of the $D_1$ hyperfine components $F = 1, 2 \rightarrow F' = 1, 2$ (see figure 2(a)). As a consequence, different transitions interact with the laser fields for different velocity classes. The buffer gas additionally causes collision-induced changes in atomic velocity (velocity-changing collisions), thus continuously mixing the velocity classes. In these conditions, optical pumping is only weakly dependent on the laser frequency within the Doppler excitation profile [15, 29].

## 3. Time-dependent Ramsey sequence

The temporal sequence of laser pulses proposed and demonstrated in this work is sketched in figure 2(b). The experiment is realised with pump and delayed probe pulses sent to the atomic vapour, while the transverse magnetic $B_\perp$ field is periodically swept in the interval $[-15$ mG, $+15$ mG$]$. To investigate the temporal Ramsey-induced narrowing of the EIA resonance, three parameters are also explored through the experiment: the duration of the pump pulse ($\tau_P$), the duration of the probe pulse ($\tau_{probe}$), and the delay between the two ($\tau_{dark}$). The experimental sequence is ideally divided in three phases, described in the following.

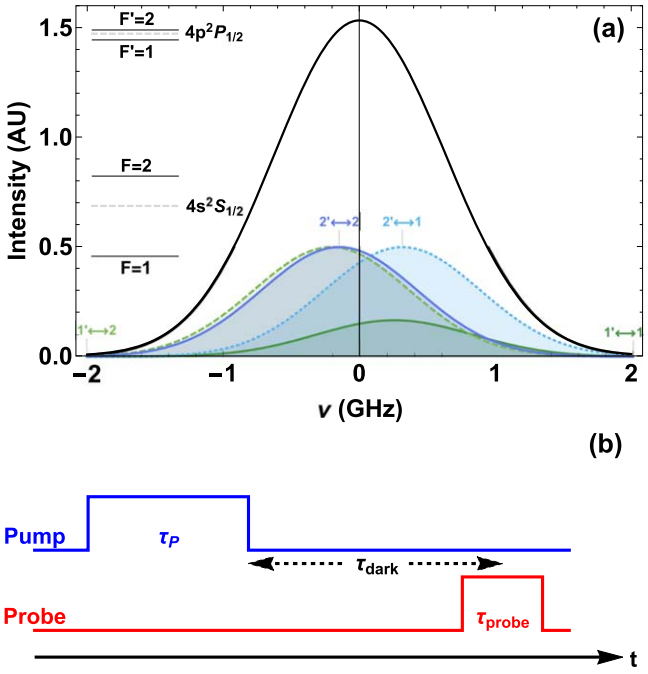


**Figure 2.** Atom-light interaction scheme. (a) Hyperfine structure of the $^{39}$K $D_1$ line at 770.1 nm, with the corresponding optical transitions line profiles. Collisional broadening with buffer gas and Doppler broadening (at 45 °C) have been taken into account. The darker areas underneath the curves show the degree of overlapping. The black line marks the resulting Doppler-broadened absorption lineshape. (b) Experimental sequence: optical pumping, free evolution in the dark, and laser probing stages.

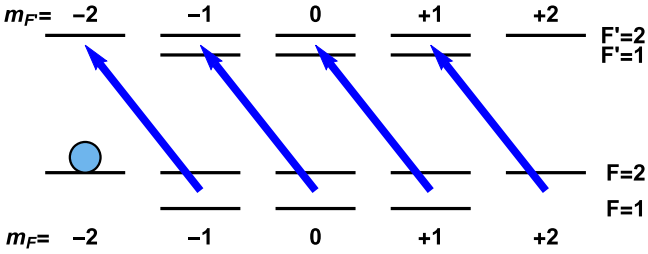


**Figure 3.** Atomic state preparation: $^{39}$K $D_1$ line $\sigma^-$ pump excitation scheme. For simplicity, the case corresponding to $B_\perp = 0$ is shown. Laser excitations are drawn between the $F = 1, 2$ levels to highlight the role of the overlapping of the hyperfine structure.

### *3.1. Atoms preparation: optical pumping*

A strong pump beam, circularly polarised ($\sigma^-$) and tuned close to the $|F = 1\rangle \rightarrow |F' = 2\rangle$ transition to empirically maximise the amplitude of the EIA (see also [15]), is used. The intense pump pulse prepares the atomic stretched state $|F = 2, m_F = -2\rangle$ (figure 3), in the presence of the weak transverse $B_\perp$.

The pump pulse duration $\tau_P$ was varied between 800 $\mu$s and 2 ms. Its optimum peak intensity was found to be 41 m W cm$^{-2}$. This corresponds to around $24I_{sat}$, where $I_{sat}$ = 1.71 mW cm$^{-2}$ is the saturation intensity of the K $D_1$ line [30]. The possibility of using such a large intensity without detrimental broadening effects is one the key features of the present work: the temporal separation between the pumping and the probing phases allows full exploitation of the pump power.

The $\sigma^-$ polarised pump produces an almost complete depletion of the $F = 1$ ground state and an efficient atomic preparation in the $|F = 2, m_F = -2\rangle$ state. This is consistent with our experimental observation that, with a single circularly polarised laser beam, only dark resonances are observed, independently of the laser detuning across the entire Doppler profile. This phenomenon is caused by the imbalance in the ground state population produced by optical pumping in Hanle configuration [29]. Also, the amplitude of the EIA resonance exhibits a broad maximum when the laser frequency is tuned around the $F = 1 \rightarrow F' = 1, 2$ transitions, in agreement with the optical pumping mechanisms outlined above.

### *3.2. Atoms free evolution: dark time*

After the optical pumping pulse, atoms are left freely evolving in the dark for a variable time $\tau_{dark}$. From this stage, at zero magnetic field $B_\perp = 0$, the conditions for EIA are produced as a consequence of the mixing between the ground state sublevels and the imbalance in the atomic population distribution realised with the initial stretched state. In addition, atomic spins precess when $B_\perp \neq 0$, giving rise to Ramsey oscillations.

To analyse the atomic evolution, we choose the quantisation axis parallel to the pump light propagation direction. The system's interaction Hamiltonian during the dark phase can be written as:

$$H_{dark} = \frac{\mu_B g_F}{\hbar} F_z B_\perp, \tag{1}$$

where $\mu_B$ is the Bohr's magneton and $F_z$ the component along $B_\perp$ of the total angular momentum operator $F$. The $|F = 2, m_F = -2\rangle$ is not an eigenstate of $H_{dark}$: the initial stretched state evolves into a coherent superposition of the $F = 2$ atomic sublevels.

At the same time, $B_\perp$ also causes the populations of the different ground sublevels to oscillate in time. This produces a periodic modulation of the population distribution, which is a fingerprint of the time-dependent Ramsey effect. During the experiments, the duration of the free evolution or 'dark' phase was varied between $\tau_{dark}$ = 12.5 $\mu$s and $\tau_{dark}$ = 2 ms, when measured from the end of the pump pulse to the middle of the probe pulse.

### *3.3. Atoms interrogation: probing*

After the delay $\tau_{dark}$, a weak counter-propagating probe pulse, also circularly polarised and at the same frequency of the pump one, probes the atomic state after its free evolution. This process is sketched in figure 4.

The probe transmission through the atomic vapour is monitored as a function of $B_\perp$, swept at a rate of 20 mG s$^{-1}$. The time scale for the $B_\perp$ field scan is significantly longer than the atomic evolution. In this condition, we can safely assume the experiment performed in condition of static magnetic field.

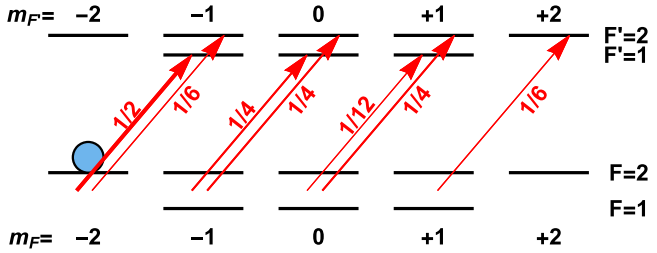


**Figure 4.** Atomic state probing: $^{39}$K $D_1$ line $\sigma^+$ probe interrogation scheme. The normalised squares of the electric dipole ($e\mathbf{r}$) matrix elements are indicated for the $\sigma^+$ $F = 2 \rightarrow F' = 1, 2$ atomic transitions leading to the formation of the EIA resonance, after optical pumping to the $|F = 2, m_F = -2\rangle$ state. The thickness of the arrows is proportional to $||\langle F', m_{F'}|e\mathbf{r}|F = 2, m_F\rangle||^2$. Note the simultaneous coupling of the $F = 2$ sublevels to the $F' = 1$ and $F' = 2$ due to the small excited state splitting of K, and the presence of buffer gas and coating. In these conditions, the state $|F = 2, m_F = -2\rangle$ has maximum coupling with the excited state. Here, the applied transverse magnetic field leads to a reduction in excitation. This is the mechanism underpinning the formation of EIA resonances.

The probe beam intensity is maintained at $I_{\text{probe}} \leqslant 5\,\text{mW cm}^{-2}$. The pulse duration $\tau_{\text{probe}}$ was varied between 10 and 150 $\mu$s. The operational conditions were empirically determined by monitoring the corresponding characteristics of the EIA peaks.

## 4. Experimental results

Typical results are shown in figure 5, for three different dark evolution durations ($\tau_{\text{dark}}$). Figures show the measured probe transmission $T_{\text{probe}}$ as a function of $B_\perp$. The Doppler transmission level was also measured, and is marked with dashed lines for comparison. This confirms a substantial decrease of probe transmission (i.e. increase of the probe absorption) at $B_\perp = 0$. This is a typical feature of EIA. For completeness, we note that detection was triggered by the pulsing of the AOMs, but not gated. Data are acquired at each cycle, and then analysed offline. Only data with the probe on at the desired magnetic field were retained and reported here.

Consistently with the mechanisms introduced in the previous sections, the EIA peak is attributed to the difference in strength of the $|F = 2, m_F\rangle \rightarrow |F' = 1, 2, m_{F'+1}\rangle$ transitions coupled by the probe beam. By averaging the couplings to the two excited states, as from figure 4, it appears that the state $|F = 2, m_F = -2\rangle$ has a stronger coupling to the excited state compared to the neighbouring Zeeman sublevels $|F = 2, m_F > -2\rangle$. Thus, the application of a transverse magnetic field ($B_\perp \neq 0$), and the consequent redistribution of the population among the Zeeman ground state sublevels, leads to a reduction of the probe absorption. This corresponds to EIA produced by transfer of population at $B_\perp = 0$.

Figure 5 also clearly demonstrates the onset of Ramsey oscillations, as a function of $\tau_{\text{dark}}$, mapped to the modulation of $T_{\text{probe}}$. This effect is overlapped to the EIA resonance

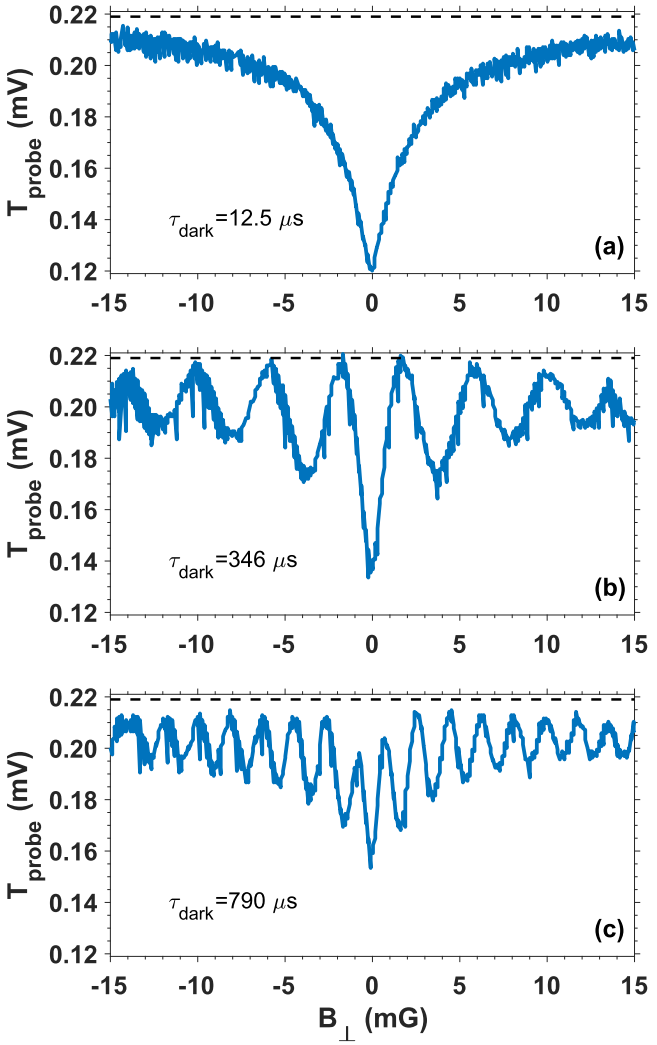


**Figure 5.** Probe transmission ($T_{\text{probe}}$) versus $B_\perp$, for different values of the delay $\tau_{\text{dark}}$ between pump and probe pulses, as indicated in the figure. Dashed lines: doppler transmission level.

(dependent on $B_\perp$, figure 5(a)), and leads to a progressive narrowing of the EIA peak, as it can be seen in figures 5(b) and (c). A similar mechanism, in presence of electromagnetically induced transparency (EIT), was reported in [23, 31].

Steep variations of the absorption levels are also obtained. For example, in the case of figure 5(b), we observe a K EIA gradient of $4.6 \times 10^{-2}\,\text{mV mG}^{-1}$, corresponding to 85 % of the total EIA resonance amplitude (see figure 5(a)) in only 1.5 mG. A similar argument gives $6.5 \times 10^{-2}\,\text{mV mG}^{-1}$ for $\tau_{\text{dark}} = 790$ $\mu$s (figure 5(c)). The corresponding value without the Ramsey narrowing is around $4 \times 10^{-3}\,\text{mV mG}^{-1}$, as obtained from figure 5(a).

The Ramsey fringes originate from the free evolution of the atomic ground state in the transverse magnetic field $B_\perp$, when the populations of the different sublevels oscillate in time. The fringes' width is predicted to scale inversely with the time delay $\tau_{\text{dark}}$ [23]. Consistently, the probe transmission $T_{\text{probe}}(B_\perp)$ exhibits an oscillatory behaviour superimposed to

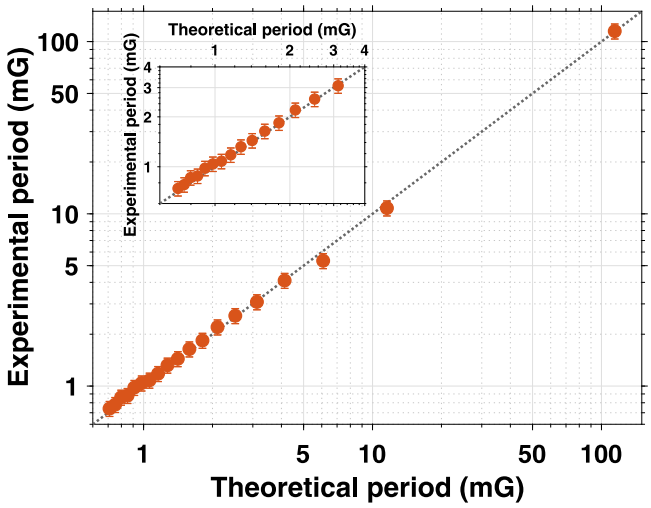


**Figure 6.** Experimental values of the Ramsey fringes period versus the theoretical prediction according to equation (2). Inset: detail of the short period data. Results are shown in terms of magnetic field units to facilitate comparison with figure 5. The dotted grey line marks the ideal correspondence between experiment and theory.

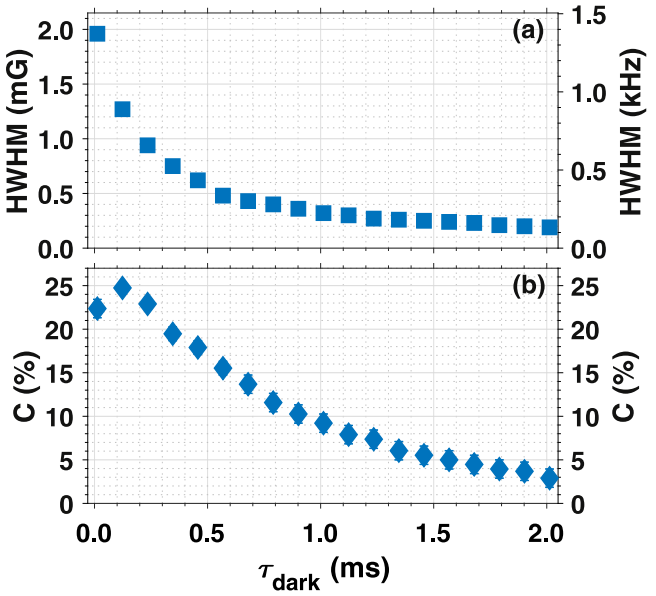


**Figure 7.** Half width at half maximum (HWHM) and contrast ($C$) of the Ramsey-narrowed EIA versus the free evolution duration $\tau_{dark}$. Error bars are concealed by markers.

EIA resonance of the form:

$$T_{probe}(B_\perp) \propto \cos\left[\frac{\mu_B B_\perp}{2\hbar}\tau_{dark}\right]. \quad (2)$$

Such fringes thus produce narrowing for increasing $\tau_{dark}$, the key feature of interest here.

Optimum EIA performance was found with the maximum available intensity for the pump probe ($I_P = 41\ mW\ cm^{-2}$). This confirms the importance of the state preparation, and the effectiveness of the proposed method in overcoming saturation issues due to intense pump beams. Contrary to previous works, increase of the pumping intensity did not produce any detrimental effects, in the explored range $\tau_P = [800\ \mu s–2\ ms]$. Accordingly, in the following, the pump duration is fixed to $\tau_P = 2$ ms. The best EIA results were obtained with a probe pulse duration of $\tau_{probe} = 25\ \mu s$. The probe power was kept in the $\mu$W region to optimise the signal, without perturbing the atomic state, as required by the Ramsey technique.

On average, experimental results for the Ramsey fringes oscillation frequency are in agreement with the predicted period within 2%, as produced by experimental uncertainties on the determination of the time $\tau_{dark}$ (figure 6).

In the following, the Ramsey fringes are used as a controllable tool for reducing the width of the EIA resonances. The Ramsey-narrowed EIA peaks are characterised in terms of contrast ($C$) and width (HWHM). The amplitude of the EIA peak $A$ and its HWHM are obtained by fitting the EIA resonances with a Lorentzian curve. Similarly to previous works with EIA (and EIT), $C$ is defined as the ratio between the amplitude $A$ of the EIA peak measured in the probe transmission:

$$A = T_{probe}(B_\perp = 0) - T_{probe}(|B_\perp| \gg 0) \quad (3)$$

and the amplitude of the Doppler absorption, measured without $B_\perp$ and with the sole probe beam. Operationally, the laser is swept through the resonance by around $\pm 1$ GHz from the $\nu_0$ resonant frequency. In summary, $C$ is given by:

$$C = \frac{A}{T_{probe}(\nu_0) - T_{probe}(\pm 1\ GHz)}. \quad (4)$$

The width and the contrast of the Ramsey EIA resonance are plotted in figure 7 as a function of the time delay $\tau_{dark}$.

Data exhibit a substantial narrowing of the EIA resonance, produced by the Ramsey fringes for longer $\tau_{dark}$. The narrowing is in agreement with the proposed Ramsey mechanism for EIA, and allows one to obtain resonances as narrow as HWHM $= 130 \pm 10$ Hz ($1.86 \times 10^{-8}$ T, as obtained from $\Delta_{Hz} = \gamma\Delta_G$, where $\gamma = 0.7\ MHz\ G^{-1}$). This demonstrates that the temporal Ramsey scheme allows one to produce EIA resonances useful for sensing and metrology.

After an initial increase, contrast shows a reduction from about $C = 25\%$ to a few percent over the range of explored $\tau_{dark}$. We interpret such a decrease as the evidence that relaxation mechanisms disturb the ground state free evolution during the dark time between the application of the pump and probe beams. The most important cause of this process is the non-ideal compensation of stray magnetic fields. Additional shielding would be required to reduce this effect. Stray magnetic fields also determine the ultimate observed linewidth. This, although controlled here by $\tau_{dark}$, could be further improved by using multiple layers of mu-metal. Notwithstanding this practical limitation of the setup, the effectiveness of the Ramsey approach with EIA is demonstrated. Compared to recent observations [15, 16], it allows a significant reduction of the EIA linewidth, well below the kHz range.

Finally, to highlight the potential for use in metrology and magnetometry—and in general to high-resolution spectroscopy—a figure of merit $F$ for characterising the EIA performance is introduced, loosely along the lines of practical

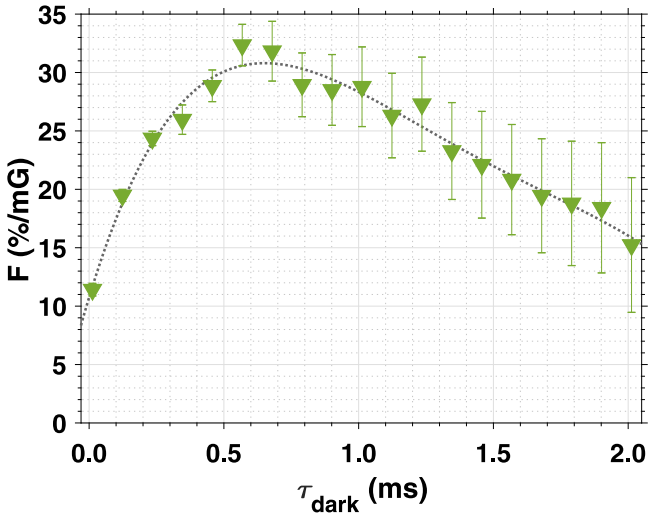


**Figure 8.** Figure of merit $F$ of the Ramsey-narrowed EIA versus $\tau_{dark}$. The dotted line is a guide to the eye.

definitions in atomic magnetometry:

$$F = \frac{C(\%)}{\mathrm{HWHM(mG)}}. \quad (5)$$

In this sense, $F$ can be interpreted as the response of the Ramsey-narrowed EIA system to a change of magnetic field. Its value is plotted against $\tau_{dark}$ in figure 8. As it is clearly seen, the interplay between the temporal Ramsey-induced narrowing of the EIA resonance and the decrease of the contrast produces a local maximum at $\tau_{dark} \approx 0.6$ ms, in the explored experimental conditions. A figure of merit F of around 32 % $\mathrm{mG}^{-1}$ is found for $\tau_{dark} = 568$ $\mu$s.

This clearly corresponds to the optimum operation point for high-resolution applications, such as for example frequency or magnetic field locking and tracking. Albeit this value depends on the details of the specific experimental setup, it could be easily identified and optimised according to the desired use.

## 5. Conclusions

In conclusion, we explored the possibility to use EIA for sensing and metrology. These applications require ultra-narrow resonances, which past work has shown to be difficult to realise in EIA. Our method relies on the preparation of a stretched state during optical pumping, its evolution in the dark in the orthogonal field, and its temporally separated probing. The time sequence of pump/free evolution/probe allows one to observe Ramsey fringes within (and outside) the EIA resonance. This leads to a significant decrease of the EIA linewidth, controllable via the duration of the free evolution in the dark. In particular, we have demonstrated that Ramsey spectroscopy of EIA resonances in a potassium vapour leads to sub-kHz fringes, as narrow as 130 Hz, currently limited by residual spurious magnetic fields.

## Acknowledgments

This work was supported by the Royal Society International Exchanges Grant 'MAGICA' (IE160163), and partially funded by the Engineering and Physical Sciences Research Council (EPSRC, EP/R011745/1).

We acknowledge discussions with Prof C Marinelli (University of Siena), and technical assistance from A Barbini, F Pardini, M Tagliaferri, and M Voliani.

## ORCID iDs

Lorenzo Lenci https://orcid.org/0000-0001-8414-4412
Luca Marmugi https://orcid.org/0000-0001-7405-5141
Ferruccio Renzoni https://orcid.org/0000-0002-4286-5323
Silvia Gozzini https://orcid.org/0000-0002-5818-6456
Alessandro Lucchesini https://orcid.org/0000-0002-8075-1722
Andrea Fioretti https://orcid.org/0000-0002-3503-5743

## References

[1] Ludlow A D, Boyd M M, Ye J, Peik E and Schmidt P O 2015 *Rev. Mod. Phys.* **87** 637–701
[2] Budker D and Romalis M 2007 *Nat. Phys.* **3** 227–234
[3] Alzetta G, Gozzini A, Moi L and Orriols G 1976 *Il Nuovo Cimento* B **36** 5–20
[4] Arimondo E and Orriols G 1976 *Lett. Nuovo Cimento* **17** 333–8
[5] Arimondo E 1996 V coherent population trapping in laser spectroscopy *Progress in Optics* vol 35 (Amsterdam: Elsevier) pp 257–354
[6] Wynands R and Nagel A 1999 *Appl. Phys.* B **68** 1–25
[7] Erhard M and Helm H 2001 *Phys. Rev.* A **63** 043813
[8] Abdel Hafiz M, Coget G, Yun P, Guérandel S, de Clercq E and Boudot R 2017 *J. Appl. Phys.* **121** 104903
[9] Affolderbach C, Stähler M, Knappe S and Wynands R 2002 *Appl. Phys.* B **75** 605–12
[10] Belfi J, Bevilacqua G, Biancalana V, Dancheva Y and Moi L 2007 *J. Opt. Soc. Am.* B **24** 1482–9
[11] Akulshin A M, Barreiro S and Lezama A 1998 *Phys. Rev.* A **57** 2996–3002
[12] Lezama A, Barreiro S and Akulshin A M 1999 *Phys. Rev.* A **59** 4732–5
[13] Dancheva Y, Alzetta G, Cartaleva S, Taslakov M and Andreeva C 2000 *Opt. Commun.* **178** 103–10
[14] Renzoni F, Zimmermann C, Verkerk P and Arimondo E 2001 *J. Opt.* B **3** S7–S14
[15] Gozzini S, Fioretti A, Lucchesini A, Marmugi L, Marinelli C, Tsvetkov S, Gateva S and Cartaleva S 2017 *Opt. Lett.* **42** 2930–3
[16] Brazhnikov D V, Ignatovich S M, Vishnyakov V I, Skvortsov M N, Andreeva C, Entin V M and Ryabtsev I I 2018 *Laser Phys. Lett.* **15** 025701
[17] Zhukov A A, Zibrov S A, Romanov G V, Dudin Y O, Vassiliev V V, Velichansky V L and Yakovlev V P 2009 *Phys. Rev.* A **80** 033830
[18] Kim H J and Moon H S 2011 *Opt. Express* **19** 168–74
[19] Grujić Z D, Mijailović M, Arsenović D, Kovačević A, Nikolić M and Jelenković B M 2008 *Phys. Rev.* A **78** 063816

[20] Gozzini S, Marmugi L, Lucchesini A, Gateva S, Cartaleva S and Nasyrov K 2011 *Phys. Rev.* A **84** 013812
[21] Kim H J and Moon H S 2012 *Opt. Express* **20** 9485–92
[22] Moon H S and Kim H J 2014 *Opt. Express* **22** 18604–11
[23] Zanon T, Guerandel S, de Clercq E, Holleville D, Dimarcq N and Clairon A 2005 *Phys. Rev. Lett.* **94** 193002
[24] Goren C, Wilson-Gordon A D, Rosenbluh M and Friedmann H 2003 *Phys. Rev.* A **67** 033807
[25] Dimitrijević J, Krmpot A, Mijailović M, Arsenović D, Panić B, Grujić Z and Jelenković B M 2008 *Phys. Rev.* A **77** 013814
[26] Renzoni F, Cartaleva S, Alzetta G and Arimondo E 2001 *Phys. Rev.* A **63** 065401
[27] Fleischhauer M, Imamoglu A and Marangos J P 2005 *Rev. Mod. Phys.* **77** 633–73
[28] Balabas M V, Karaulanov T, Ledbetter M P and Budker D 2010 *Phys. Rev. Lett.* **105** 070801
[29] Gozzini S, Cartaleva S, Lucchesini A, Marinelli C, Marmugi L, Slavov D and Karaulanov T 2009 *Eur. Phys. J.* D **53** 153–61
[30] Hanley R K, Gregory P D, Hughes I G and Cornish S L 2015 *J. Phys. B: At. Mol. Opt. Phys.* **48** 195004
[31] Guerandel S, Zanon T, Castagna N, Dahes F, de Clercq E, Dimarcq N and Clairon A 2007 *IEEE Trans. Instrum. Meas.* **56** 383–7